

## Superlattice effects induced by atomic ordering on $\text{Ga}_x\text{In}_{1-x}\text{P}$ Raman modes

A. Hassine, J. Sapriel, and P. Le Berre

*France Telecom, Centre National d'Etudes des Télécommunications, Paris B, Laboratoire de Bagneux, 196 Avenue H. Ravera, 92225 Bagneux Cedex, France*

M. A. Di Forte-Poisson

*Thomson-CSF, Laboratoire Central de Recherches, 91404 Orsay Cedex, France*

F. Alexandre and M. Quillec

*France Telecom, Centre National d'Etudes des Télécommunications, Paris B, Laboratoire de Bagneux, 196 Avenue H. Ravera, 92225 Bagneux Cedex, France*

(Received 16 January 1996)

A polarized Raman scattering study is undertaken in order to investigate the atomic ordering in (001)-oriented  $\text{Ga}_{0.51}\text{In}_{0.49}\text{P}$  layers lattice matched to GaAs and preliminarily characterized by photoluminescence. The superlattice structure of trigonal symmetry which results from ordering manifests itself through phonon mode modifications. Several new modes are detected and their frequency and intensity behaviors are properly analyzed. In addition to the folded longitudinal-acoustic mode on Raman spectra, we observed the folded transverse-acoustic mode. Both folded acoustic modes display narrow lines ( $\sim 10 \text{ cm}^{-1}$ ) superposed to the disorder-induced acoustic bands DALA and DATA of the alloy. In the "optical mode" frequency range one clearly observes a doubling of the longitudinal GaP-type and InP-type modes, never reported before to our knowledge. The magnitude of the splitting between the two components of the LO doublet is measured precisely in the case of GaP-type modes and is an increasing function of the atomic ordering degree. So it is with intensities of the TO modes which become Raman active due to the trigonal symmetry. Finally the "valley depth" which had been empirically assigned as a significant parameter of the atomic ordering degree, is now precisely interpreted in the light of the whole Raman study. [S0163-1829(96)07528-5]

### I. INTRODUCTION

Atomic ordering in an alloy results in the spontaneous formation of a short-period superlattice along a particular crystallographic direction.<sup>1,2</sup> This phenomenon has been observed in nearly all alloys systems under certain conditions of growth. It is indeed a topic of increasing interest for fundamental studies and its control is crucial for electronic and photonic devices. Atomic ordering is predicted and experimentally observed to induce a reduction in the band-gap energy of III-V alloys, notably  $\text{Ga}_{0.51}\text{In}_{0.49}\text{P}$  (hereafter referred to as  $\text{GaInP}_2$ ) lattice matched to (001)-oriented GaAs substrates.

In a disordered  $\text{GaInP}_2$  crystal of symmetry  $F\bar{4}3m$  the cations are randomly positioned on the group-III sublattice of the zinc-blende structure. If order is assumed, a new trigonal crystal is created, along one of the four threefold rotation axes [111] of the subgroup  $R3m$  (CuPt-type structure). Atomic ordering gives rise to a superlattice of alternating Ga-rich ( $\text{Ga}_{1+\delta}\text{In}_{1-\delta}\text{P}_2$ ) and In-rich ( $\text{Ga}_{1-\delta}\text{In}_{1+\delta}\text{P}_2$ ) alloy monolayers perpendicular to this axis. The parameter  $\delta$  ( $0 < \delta < 1$ ) characterizes the degree of atomic ordering.

Raman scattering is a useful and nondestructive tool to characterize crystals and microstructures. A great deal of investigation has been devoted to III-V artificial superlattices (particularly the GaAs/ $\text{Ga}_x\text{Al}_{1-x}\text{As}$  system) and IV-IV superlattices (as Si/GeSi). In these structures, superlattice effects have been evidenced on the "folding" of the acoustic branches as well as on the optical modes whose number in-

creases because of the multiplication of the unit cell.<sup>3,4</sup> As to ordered  $\text{GaInP}_2$  alloys, the only superlattice feature observed in the Raman spectra, so far, is the appearance of a small peak around  $200 \text{ cm}^{-1}$ . This peak was attributed to the LA mode at the  $L$  point of the Brillouin zone, which becomes Raman active as a consequence of the unit cell doubling.<sup>5</sup> In this study, in addition to this mode which is now fully characterized, we point out several other modes in the Raman spectra due to the superlattice effect and the trigonal symmetry which are unambiguously related to the atomic ordering and are characteristic of its degree. A satisfactory interpretation of the "valley depth," which remained so far a phenomenological parameter, assigned<sup>5</sup> to the ordering, is here given in term of the order and symmetry transformations.

### II. SAMPLE PREPARATION AND PRELIMINARY ORDERING CHARACTERIZATION

In the present paper several (001)  $\text{GaInP}_2$  samples lattice matched to GaAs are investigated. All samples, though corresponding to nearly the same nominal composition (51% and 49% for Ga and In, respectively), actually differ by the atomic ordering degree  $\delta$ . The GaAs substrate has been misoriented by  $\sim 2^\circ$  in the  $[\bar{1}10]$  direction in order to allow the growth of single variant<sup>6</sup>  $\text{GaInP}_2$  with atomic ordering along  $[\bar{1}11]$ .

Ordered crystals display a reduction  $\Delta E_g$  of the electronic band gap  $E_g$  corresponding to the zinc-blende structure and simultaneously a splitting  $\delta E_v$  of the valence band occurs.<sup>7</sup>

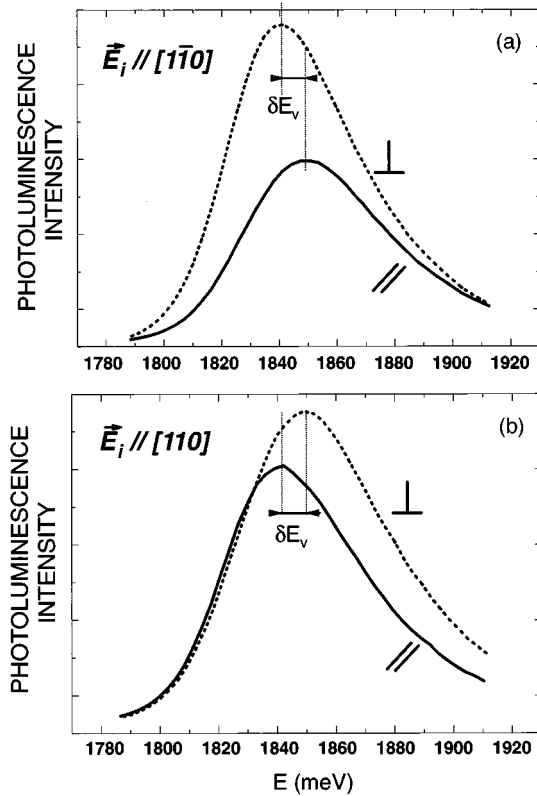


FIG. 1. Polarized PL emission at room temperature on our most ordered sample. Following Ref. 7,  $\vec{E}_i$  is the polarization of the incident light direction which can be along  $[\bar{1}10]$  (a) or along  $[110]$  (b);  $\parallel$  and  $\perp$  correspond to the emitted photoluminescence polarization direction with respect to  $\vec{E}_i$ .  $\delta E_v$  the valence-band splitting. This kind of experiment allows to discriminate between the two nonequivalent directions  $[110]$  and  $[\bar{1}10]$  (exciting light  $\lambda=5145$  Å);  $[110]$  being the direction perpendicular to the atomic ordering axis  $[\bar{1}11]$ .

The lattice mismatch between the  $\text{GaInP}_2$  layers and the GaAs substrate was measured by means of high-resolution x-ray diffractometry at room temperature, and was found below  $6 \times 10^{-4}$ . We could therefore neglect the influence of compositional fluctuations and the resulting strain, on the band gap and the band edges. Samples grown by different epitaxial techniques [liquid-phase epitaxy (LPE),<sup>8</sup> chemical beam epitaxy (CBE),<sup>9</sup> and metalorganic chemical vapor deposition<sup>10</sup> (MOCVD)], were available for the purpose of this study. They displayed various degrees of ordering.

Both the shrinkage  $\Delta E_g$  and the splitting  $\delta E_v$  can be precisely measured through photoluminescence (PL) experiments. The larger the  $\Delta E_g$  and  $\delta E_v$  values, the highest the atomic ordering in the crystal. In the ordering range of our samples we found approximately  $\Delta E_g \sim 5 \delta E_v$  in good agreement with Ref. 11. In the following, we will actually take  $\delta E_v$  as the characteristic ordering parameter since its measurement is straightforward from polarized PL in the particular geometries of Fig. 1. Besides, PL allows us to discriminate between the two nonequivalent axes  $[110]$  and  $[\bar{1}10]$  in the ordered trigonal structure along  $[\bar{1}11]$ . Accordingly, PL is here used as a suitable tool for both preliminary ordering characterization and crystal orientation of the samples, before our proper Raman study.

### III. RAMAN INVESTIGATION OF THE ATOMIC ORDERING

The experiments are performed at 80 K and 300 K mainly with the argon-ion laser line 5145 Å. The Raman signal is detected by a U1000 double monochromator from Jobin-Yvon, the same one which has been used for the preliminary PL characterization of the samples.

As Raman experiments are performed on our (001) samples in the backscattering geometry, the phonons involved exclusively propagate along  $z$  the  $[001]$  axis of the zinc-blende structure, and light is always polarized in the  $xy$  plane. The real structure of the crystal being trigonal along  $[\bar{1}11]$ ; ( $Z$  axis), only two kinds of Raman modes can be observed: the unidimensional  $A_1(Z)$  and bidimensional  $E(X,Y)$  modes<sup>12,13</sup> which obviously correspond to the longitudinal and transverse modes, respectively.

For modes under  $220 \text{ cm}^{-1}$  (acoustic branch range) the experiments have been performed under vacuum to avoid spurious light from air Raman lines. It is worthwhile pointing out that all samples whatever their atomic ordering degree exhibit the same kind of feature in this range. Actually in the geometries corresponding to parallel polarizations of the incident and diffracted light, one can clearly observe the disorder-induced acoustic longitudinal band (DALA) and disorder-induced acoustic transverse band<sup>14</sup> (DATA) corresponding to the same alloy  $\text{GaInP}_2$ . These Raman bands correspond to the zone edge of the LA and TA branches, respectively, where the density of phonon states is high, and peak around 80 and  $200 \text{ cm}^{-1}$ . In addition to the DALA and DATA, one can observe in “ordered” samples the superposition of rather narrow lines at  $68$  and  $208 \text{ cm}^{-1}$  which we assign to the folded transverse acoustic mode (FTA) and folded longitudinal acoustic mode<sup>15</sup> (FLA), as a consequence of the doubling of the unit cell in the  $[\bar{1}11]$  direction [Fig. 2(a)]. By subtracting the spectra corresponding to an ordered and disorder sample one can clearly evidence these two modes whose linewidth at half maximum is about  $10 \text{ cm}^{-1}$  [Fig. 2(b)]. We identify the FLA as an  $A_1$  mode and the FTA as an  $E$  mode. Both modes are allowed. The FLA is observed only for parallel polarizations of the incident and scattered light. It cancels for orthogonal polarizations. Its intensity increases for increasing values of  $\delta E_v$  (see Fig. 3). As to the FTA, it is seen for all geometries but its intensity is clearly smaller.

In the disordered alloy  $\text{GaInP}_2$  display a two-mode-behavior<sup>16</sup> with  $\text{LO}_1$  (GaP-type) and  $\text{LO}_2$  (InP-type). Besides the longitudinal modes the transverse  $\text{TO}_2$  (InP-type) is observed as a small mode, even in (100) samples, in spite of the fact that it is not allowed. As to the  $\text{TO}_1$  (GaP-type) it is hidden by  $\text{LO}_2$  since it is at the same time Raman inactive in (100) crystal and at a frequency very close to  $\text{LO}_2$  (just above it<sup>17</sup>).

In the trigonal system whose axes  $X, Y, Z$  are parallel to  $[\bar{1}1\bar{2}]$ ,  $[110]$ , and  $[\bar{1}11]$ , respectively, the only nonzero elements of the Raman tensor corresponding to  $A_1(Z)$  are  $A_1^{XX} = A_1^{YY} = c$  and  $A_1^{ZZ} = d$ . Yet, the most suitable reference system for the Raman scattering experiments is the zinc blende one  $x, y, z$ . Following the textbook of Poulet and Mathieu<sup>12</sup> one finds for the intensities of the  $A_1$  modes, after a few tensor manipulations:

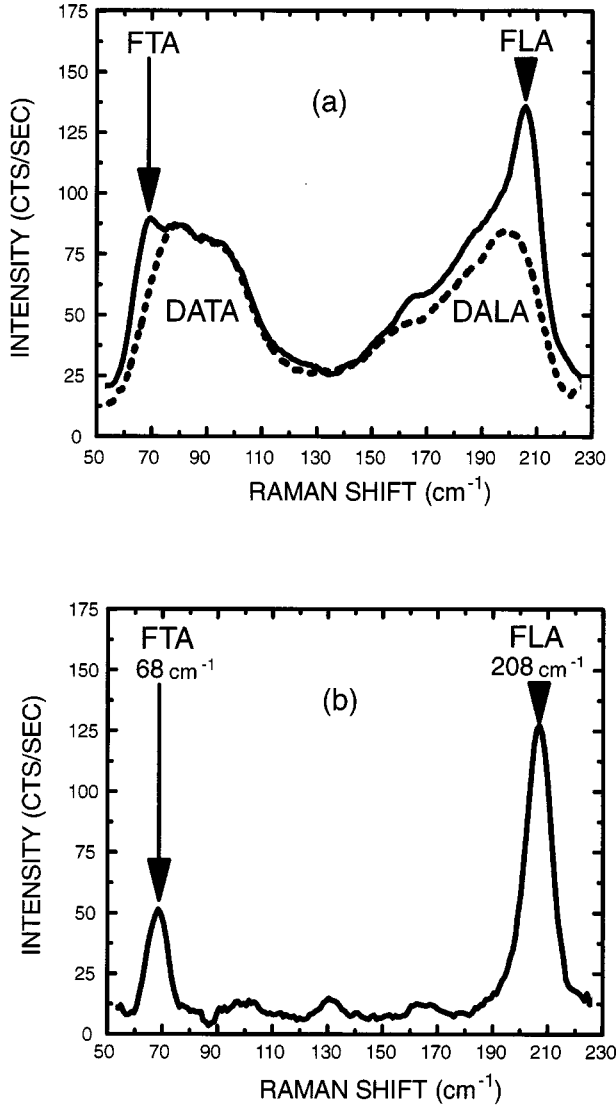


FIG. 2. (a) Comparison between the most disordered (dashed line) and the most ordered (full line) among the samples; FTA and FLA lines are superposed to the disordered activated modes DALA and DATA of the alloy GaInP<sub>2</sub>. (b) The result obtained after subtraction of the two spectra of (a). The FTA and FLA are two well-defined peaks of  $\sim 10$  cm<sup>-1</sup> width at half maximum. All spectra are obtained at 80 K in order to reduce the second-order Raman lines.

$$I_{\parallel} = C[(2c + d) + (c - d)\sin 2\theta]^2, \quad (1)$$

$$I_{\perp} = C(c - d)^2 \cos^2 2\theta. \quad (2)$$

In Eqs. (1) and (2),  $\theta$  is the angle of the incident light polarization with the  $x$  axis in the  $xy$  plane, the intensities  $I_{\parallel}$  and  $I_{\perp}$  correspond to scattered light polarizations parallel or perpendicular to the incident one, respectively, and  $C$  is a constant. Clearly  $I_{\parallel}(\theta=0) = I_{\parallel}(\theta=\pi/2)$ , though  $I_{\parallel}(\theta=\pi/4) \neq I_{\parallel}(\theta=3\pi/4)$ ; i.e.,  $x$  and  $y$  axes are equivalent contrary to the directions  $x'$  and  $y'$  with  $x' \parallel [110]$  and  $y' \parallel [\bar{1}10]$  corresponding then to  $\theta = \pi/4$  and  $3\pi/4$ , respectively. These results can be directly deduced by symmetry considerations. It is worthwhile pointing out also that  $I_{\perp}^{x'y'}$  is null for all  $A_1$  modes. For  $c = d$ , one finds  $I_{\parallel}$  constant and

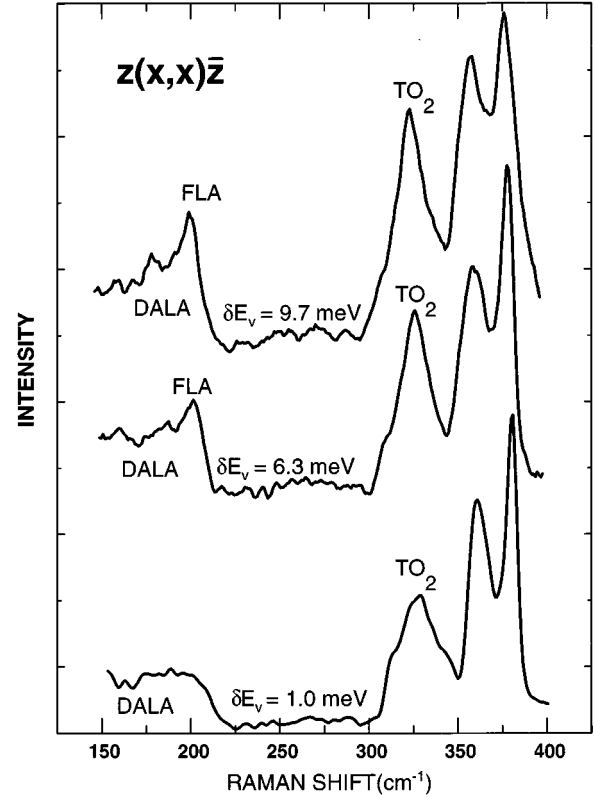


FIG. 3. Raman spectra for samples corresponding to different values of  $\delta E_v$  showing the increase of FLA and TO<sub>2</sub> intensities as a function of the atomic ordering degree.

equal to  $39 Cc^2$ , though  $I_{\perp}$  is equal to zero for all  $\theta$  values. Such intensity behavior is indeed observed in the case of the FLA mode. For a disordered alloy  $d = -2c$  (Raman selection rules of the LO in a cubic  $43m$  crystal).

In the most disordered sample, obtained by LPE one observes the spectrum (lower curve) of Fig. 4 in the geometry  $z(y'y')\bar{z}$  [in this notation, the symbols within (outside)

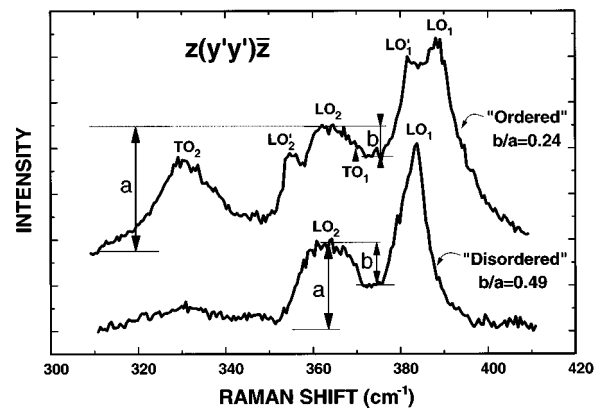


FIG. 4. Comparison between the two extreme samples ( $\delta E_v = 1$  meV for the lower spectrum and  $\delta E_v = 9.7$  meV for the upper one). One can notice, for the sample corresponding to  $\delta E_v = 9.7$  meV: (a) The splitting of the LO<sub>1</sub> and LO<sub>2</sub> modes (respectively, GaP-type and InP-type) into LO<sub>1</sub> LO<sub>1</sub>' and LO<sub>2</sub> LO<sub>2</sub>' doublets, (b) the increase of the TO<sub>2</sub> mode, (c) the reduction of the valley depth  $b/a$  ratio due to the TO<sub>1</sub> Raman activity and the doubling of the LO<sub>1</sub>.

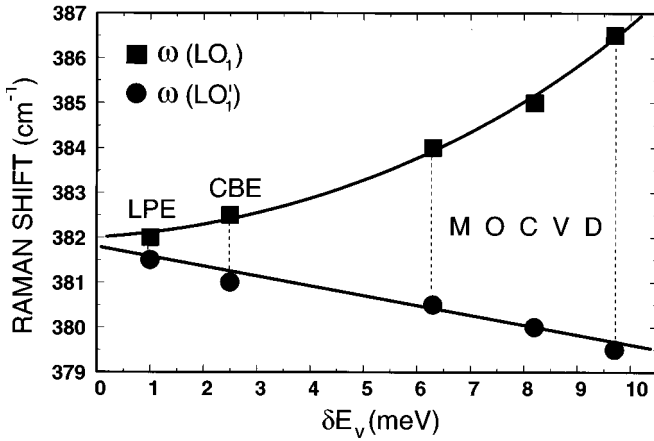


FIG. 5. Room-temperature Raman shifts of the GaP-type doublet components  $LO_1$ - $LO_1'$  as a function of the valence-band splitting  $\delta E_v$  in five samples grown by different techniques. The  $LO_1$  mode has a zinc-blende-structure-type mode, i.e., it cancels for incident and scattered light polarizations parallel to  $x$  axis (or  $y$ ).

the parameters indicate the radiation polarization (wave vectors)]. In the case of “atomic ordering,” there is a splitting of the optical modes, due to the superlattice effect. For instance, one can see (upper spectrum of Fig. 4) in the same  $z(y'y')\bar{z}$ , a doubling of the LO of the GaP and InP types. Additional  $A_1$  modes appear at lower frequencies with different Raman tensor elements  $c$  and  $d$ . Now, we observe  $LO_1$  and  $LO_1'$  for the GaP-type and  $LO_2$  and  $LO_2'$  of the InP-type. These frequency splittings  $LO_1$ - $LO_1'$  and  $LO_2$ - $LO_2'$  increase with the ordering  $\delta$ . According to our investigations the highest frequency modes  $LO_1$  and  $LO_2$  (contrary to  $LO_1'$  and  $LO_2'$ ) have selection rules very similar to those correspond-

ing to the completely random alloy of the cubic zinc blende. As a matter of fact, they mostly cancel for parallel polarizations  $xx$  or  $yy$ , though the lowest-frequency mode is clearly dominant in these scattering geometries and its peak position can be precisely measured, accordingly. We have plotted the frequency variations of  $LO_1$  and  $LO_1'$  as a function of  $\delta E_v$  (see Fig. 5).

Thus we found the ratio  $c/d = -1/2$  for both  $LO_1$  and  $LO_2$  (zinc-blende-type modes). Concerning the most ordered sample ( $\delta E_v = 9.7$  meV) we measured  $c/d = 3$  and  $c/d = -0.17$  for  $LO_1'$  and  $LO_2'$  (ordering modes), respectively. These ratios remain constant as a function of temperature. As to  $LO_1'$  we observe a large increase of its intensity as the temperature is lowered. Actually, for this mode both  $c$  and  $d$  undergo an enlargement of a factor 5 between room temperature and 80 K, as can be noticed on Fig. 6. This resonance behavior which affects only  $LO_1'$  has not yet found a satisfactory explanation.

In ordered samples we observe an increase of the  $TO_1$  and  $TO_2$  modes, of the GaP-type and InP-type, respectively. This behavior is striking for  $TO_2$  while  $TO_1$  is detected as a high-frequency shoulder of  $LO_2$  for the ordered sample of Fig. 4.

We can now simply interpret the “valley depth” parameter  $b/a$  which has been empirically correlated to the gap reduction of the  $GaInP_2$  sample, i.e., to the ordering. Obviously both the doubling of the  $LO_1$  mode and the Raman activation of  $TO_1$  which occur for ordered crystals contribute to the reduction of the valley depth ratio; thus one measures a reduction from 0.49 to 0.24 between the most disorder and the most ordered samples (Fig. 4). Similarly, the broadening of the GaP-like and the InP-like LO modes observed by Kondow *et al.*<sup>18</sup> is an effect of the splitting of these modes into two components which are unresolved in their experiments.

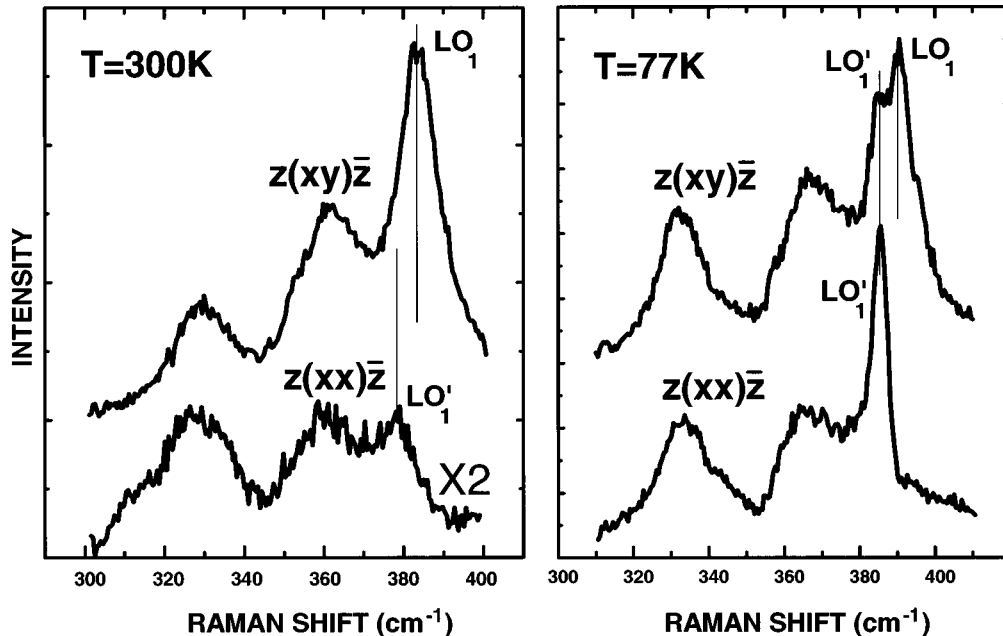


FIG. 6. Raman scattering in a  $GaInP_2$  sample with atomic ordering ( $\delta E_v = 9.7$  meV) at 300 and 77 K for the scattering configurations  $x(xy)\bar{z}$  and  $z(xx)\bar{z}$ . One can notice that  $LO_1$  completely disappears for  $z(xx)\bar{z}$  (same selection rules as in a random alloy of the zinc-blende structure) and that  $LO_1'$  intensity strongly increases at low temperatures.

#### IV. DISCUSSION AND CONCLUSION

Until only a few years ago, it was generally admitted that the atomic arrangement in III-V alloy semiconductors is random on each sublattice. The recent discovery of “atomic ordering” has completely renewed this old conception. It is now believed that an effective control of this peculiar arrangement which strongly depends on the epitaxial growth conditions (growth rates, substrate temperature and orientation, and ratio of III-V elements), would have the potential for providing materials for improved devices for microelectronic and optoelectronic applications. We have shown in the case of GaInP<sub>2</sub> that this atomic ordering, which has been characterized by PL on every sample, appears as modifications of the lattice phonon modes which we evidenced by means of Raman scattering. The mode at 208 cm<sup>-1</sup> has been now unambiguously assigned to the FLA mode as its intensity increases with increasing ordering. Additional Raman modes have been also clearly observed whose frequencies and selection rules can be predicted by elemental theoretical considerations particularly concerning the symmetry. A FTA mode of *E* symmetry appears in the low-frequency part of the ordered samples. Superlattice effects also manifest themselves through the doubling of the longitudinal-optical GaP-type and InP-type modes. All these modes correspond to the trigonal A<sub>1</sub> symmetry.

The frequency shift between the two components of each (GaP-type and InP-type) doublet is an increasing function of the atomic ordering degree in good agreement with our first investigations from simple lattice dynamics models. As to the TO<sub>1</sub> and TO<sub>2</sub> modes (of GaP-type and InP-type) they become Raman-active *E* modes due to the cubic-trigonal

transition and their intensities increase with increasing values of  $\delta E_v$ .

Even the so-called “valley depth” parameter *b/a* can be interpreted now in the light of this thorough Raman study which can be extended to many other materials since the phenomenon of atomic ordering has been observed in nearly all III-V and II-VI systems. So far, TEM experiments have been preferentially used to characterize atomic ordering in alloys. It is worthwhile pointing out that the Raman scattering, in comparison, offers the clear advantage of a nondestructive, quantitative (even the degree of ordering can be evaluated from the splitting of optical modes) and versatile method, related to both electronic and phonon properties of the ordered superstructure under investigation. Indeed, Raman investigations can be easily coupled to complementary PL measurements<sup>19,20</sup> or Brillouin scattering experiments,<sup>21</sup> using the same experimental setup.

Today’s better understanding of the ordering process allows the growth of both more ordered and more disordered layers by proper selection of the epitaxy parameters. Actually, *E<sub>g</sub>* values of our samples ranged between 1.92 and 1.85 eV at room temperature. Since recent publications<sup>22,23</sup> claim a maximum band-gap reduction of 470 meV in GaInP<sub>2</sub> one can expect the availability of new superlattice structures in the future with a much higher compositional modulation, to extend the range of the present investigations.

#### ACKNOWLEDGMENT

It is a pleasure to thank G. Leroux for preliminary x-ray characterizations.

- 
- <sup>1</sup>A. Gomyo, T. Suzuki, and S. Iijima, Phys. Rev. Lett. **60**, 2645 (1988).
- <sup>2</sup>P. Bellon, J. P. Chevalier, E. Dupont-Nivet, C. Thiebaut, J. P. Andre, and G. P. Martin, Appl. Phys. Lett. **52**, 567 (1988).
- <sup>3</sup>C. Colvard, R. Merlin, M. V. Klein, and A. C. Gossard, Phys. Rev. Lett. **45**, 298 (1980).
- <sup>4</sup>J. Sapriel and B. Djafari Rouhani, Surf. Sci. Rep. **10**, 189 (1989), and references therein.
- <sup>5</sup>T. Suzuki, A. Gomyo, S. Iijima, K. Kobayashi, S. Kawata, I. Hino, and T. Yuasa, Jpn. J. Appl. Phys. **27**, 2098 (1988).
- <sup>6</sup>T. Suzuki, A. Gomyo, and S. Iijima, J. Cryst. Growth **93**, 396 (1988).
- <sup>7</sup>A. Mascarenhas, S. Kurtz, A. Kibbler, and J. M. Olson, Phys. Rev. Lett. **63**, 2108 (1989).
- <sup>8</sup>O. Ueda, M. Hoshino, M. Takechi, M. Ozeki, T. Kato, and T. Matsumoto, J. Appl. Phys. **68**, 4268 (1990).
- <sup>9</sup>G. B. Stringfellow and G. S. Chen, J. Vac. Sci. Technol. B **9**, 2182 (1991).
- <sup>10</sup>A. Gomyo, T. Suzuki, K. Kobayashi, S. Kawata, and I. Hino, Appl. Phys. Lett. **50**, 673 (1987).
- <sup>11</sup>S. H. Wei and A. Zunger, Appl. Phys. Lett. **64**, 757 (1994).
- <sup>12</sup>H. Poulet and J. P. Mathieu, *Spectres de Vibration et Symétrie des Cristaux* (Gordon & Breach, Paris, 1970).
- <sup>13</sup>W. Hayes and R. Loudon, *Scattering of Light by Crystals* (Wiley, New York, 1978).
- <sup>14</sup>B. Jusserand and J. Sapriel, Phys. Rev. B **24**, 7194 (1981).
- <sup>15</sup>J. Sapriel, in *Interaction of Light with “Folded” Acoustic Waves in Semiconductor Superlattices*, Proceedings of the International School of Physics “Enrico Fermi,” Course CXVII, Varenna, edited by A. Stella (North-Holland, Amsterdam, 1993), p. 313. See particularly Fig. 14 corresponding to a short-period GaAs/AlAs superlattice, the FLA modes are then superposed to the DALA and DATA of the Ga<sub>0.5</sub>Al<sub>0.5</sub>As mean alloy (a situation similar to ordered GaInP<sub>2</sub>).
- <sup>16</sup>B. Jusserand and S. Slempek, Solid State Commun. **49**, 95 (1984).
- <sup>17</sup>T. Kato, T. Matsumoto, and T. Ishida, Jpn. J. Appl. Phys. **6**, 983 (1988).
- <sup>18</sup>M. Kondow, H. Kakibayashi, S. Minagawa, Y. Inoue, T. Nishino, and Y. Hamakawa, Appl. Phys. Lett. **53**, 2053 (1988).
- <sup>19</sup>J. Sapriel, J. Chavignon, and F. Alexandre, Appl. Phys. Lett. **52**, 1970 (1988).
- <sup>20</sup>A. Hassine, J. Sapriel, M. Nunez, P. Le Berre, P. Legay, F. Alexandre, G. Post, and G. Leroux, Mater. Sci. Eng. B **28**, 151 (1994).
- <sup>21</sup>A. Hassine, J. Sapriel, P. Le Berre, P. Legay, F. Alexandre, and G. Post, J. Appl. Phys. **77**, 6569 (1995).
- <sup>22</sup>K. A. Mäder and A. Zunger, Phys. Rev. B **51**, 10 462 (1995).
- <sup>23</sup>P. Ernst, C. Geng, F. Scholz, H. Schweizer, Y. Zhang, and A. Mascarenhas, Appl. Phys. Lett. **67**, 2347 (1995).